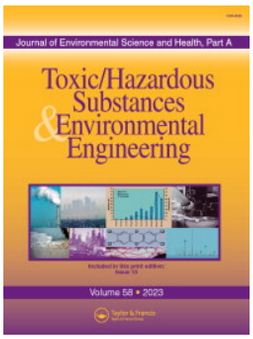

Taylor & Francis
Taylor & Francis Group

Journal of Environmental Science and Health, Part A
Toxic/Hazardous Substances and Environmental Engineering

ISSN: (Print) (Online) Journal homepage: https://www.tandfonline.com/loi/lesa20

In situ capping of silver nanoparticles with cellulosic matrices from wheat straws in enhancing their antimicrobial activity: Synthesis and characterization

Shappo Tlou, Evans Suter, Mitema Alfred, Hilary Rutto & Wesley Omwoyo

To cite this article: Shappo Tlou, Evans Suter, Mitema Alfred, Hilary Rutto & Wesley Omwoyo (21 Sep 2023): In situ capping of silver nanoparticles with cellulosic matrices from wheat straws in enhancing their antimicrobial activity: Synthesis and characterization, Journal of Environmental Science and Health, Part A, DOI: 10.1080/10934529.2023.2260295

To link to this article: https://doi.org/10.1080/10934529.2023.2260295

Published online: 21 Sep 2023.

JOURNAL OF ENVIRONMENTAL SCIENCE AND HEALTH, PART A
https://doi.org/10.1080/10934529.2023.2260295

In situ capping of silver nanoparticles with cellulosic matrices from wheat straws in enhancing their antimicrobial activity: Synthesis and characterization

Shappo Tlou[a], Evans Suter[b], Mitema Alfred[c], Hilary Rutto[b], and Wesley Omwoyo[a]

[a]Department of Chemistry, Vaal University of Technology, Vanderbijlpark, South Africa; [b]Department of Chemical Engineering, Vaal University of Technology, Vanderbijlpark, South Africa; [c]Department of Biotechnology, Vaal University of Technology, Vanderbijlpark, South Africa

ABSTRACT

Silver nanoparticles have gained worldwide attention in the scientific community due to their high antimicrobial activity. However, they tend to agglomerate and lose their shape and properties, thus capping agents necessary to protect their shapes, sizes, and properties. To enhance their antimicrobial activity, this research aimed to cap silver nanoparticles with cellulosic matrices from wheat straws. The wheat straw was delignified with 6% HNO_3, and the residual was treated with 1% NaOH and NaClO: CH_3COOH (1:1), then used to synthesize cellulose nanocrystals *via* acid hydrolysis. AgNPs were incorporated into the CPC and CNCs by in-situ synthesis using $NaHB_4$ as the reducing agent. Fourier Transform Infrared, Scanning Electron Microscopy, and X-ray diffraction were used to investigate their features. The findings exhibited crystallinity increased with subsequent treatments, according to XRD analysis. Ultraviolet-visible, FTIR, TEM, and XRD analysis confirmed the capping of AgNPs onto the cellulosic materials. Antibacterial activity against *Staphylococcus aureus* and *Escherichia coli,* with CNCs-AgNPs composite, exhibited higher activity compared to CPC-AgNPs composite due to the increased surface area and excellent binding on the surface of the composite.

ARTICLE HISTORY
Received 10 May 2023
Accepted 6 September 2023

KEYWORDS
Acid hydrolysis; cellulose nanocrystals; composite; reducing agent; capping

Introduction

Silver nanoparticles have gained worldwide attention in the scientific community due to their high antimicrobial activity.[1–6] They tend to agglomerate and lose their shape and properties; thus, capping agents protect their shapes, sizes, and properties.[7,8] Synthetic capping agents are not environmentally friendly; therefore, biopolymers occurring naturally in bulk and less expensive have gained more attention.[9–11] Cellulose has an annual productivity of 7.5 x 10^{10} tonnes, and this shows that it is the most abundant natural biopolymer and regenerates itself through photosynthesis, making it inexhaustible.[12,13] Cellulose is the most essential plant element, representing one-third of the plant fiber.[14–18] Cellulose nanomaterials are a new sub-class of biomaterials with unique properties.[12,19–22]

Wheat straws are an abundant source of cellulose at meager costs.[13] Its structure mainly consists of 15-18% lignin38-42%, 34-40% hemicellulose, and cellulose.[13,23–25] This shows that wheat straws are not only abundant but contain more significant amounts of cellulose than any other sources. The extraction of cellulose from plant materials involves delignification and bleaching.[26–28]

One of the most distinguishing features of cellulose is that each monomer has three hydroxyl groups.[29] The capacity of these hydroxyl groups to form hydrogen bonds is critical in creating fiber structure and semi-crystalline packing, which determines the crucial physical characteristics of these highly cohesive materials.[12] These chemical transformations are performed to increase the performance and ability of nano cellulose-based materials to be processed.[12,30–33] Organic antimicrobials have limited application in the health, textile, medical, and other fields thus efficiency and applicability are determined by various criteria, including their chemical characteristics, mode of action, and the unique demands of these diverse applications.[34–37]

Silver nanoparticles have high antibacterial action, affecting Deoxyribonucleic acid (DNA) replication and the collapse of proton motive force across the cytoplasmic membrane of microbes.[38–40] Silver has become a study focus due to its low toxicity in humans. Its derivatives demonstrated that they are promising materials for the functionalizing and favorable features to address the antibacterial studies.[34,41–43]

This research capped silver nanoparticles with cellulosic matrices from wheat straws to enhance their antimicrobial activity. The capping conditions and the primary characteristics of silver nanoparticles were investigated. Capping AgNPs with CPC and CNCs increased their properties and improved the antibacterial properties.

CONTACT Evans Suter esuter78@gmail.com Department of Chemical Engineering, Vaal University of Technology, Private Bag X021, Vanderbijlpark, South Africa.

Materials and methods

Materials

The wheat straw, an agricultural waste, was collected from the field and placed into black polythene bags during harvesting season in February 2019 in Narok County, Kenya. Analytical grade chemicals and reagents from Sigma Aldrich, Merck, South Africa (Nitric acid (HNO_3 ≥98.99%), absolute ethanol (C_2H_5OH >99.9%), Sodium Borohydride, $NaHB_4$ (≥98.0%), sodium hypochlorite (NaOCl ≥25%), urea ($CO(NH_2)_2$ ≥99%), sulfuric acid (H_2SO_4 ≥99.9%), acetic acid (CH_3COOH ≥99.9%), Silver nitrate ($AgNO_3$>99%), sodium hydroxide (NaOH ≥98%), and acetone $(CH_3)_2CO$ ≥99.9%), Luria Broth, and Luria Agar broth) were used. Distilled water was obtained from Vaal University of Technology distillation column.

Isolation of cellulose, synthesis of cellulose nanocrystals and silver nanoparticles, and their nanocomposites

Extraction of chemically purified cellulose (CPC) from wheat straw

The collected wheat straw was rinsed with distilled water, sun-dried for 24 h, ground using a coffee miller, and sieved through double mesh sieves (<50 µm). The resultant material was dried in an oven for approximately 8 h at 105 °C and kept at room temperature in airtight polythene bags. The fine powder (40.01 g) was transferred into a one-neck round bottom flask. Approximately 400 mL, 6% HNO_3 was poured cautiously into the fine powder and onto a hot water bath set at 90 °C for 2 h and continuously stirred to ensure homogeneity. The resultant solid was filtered through vacuum filtration and washed three times with deionized water. The recovered solid was pretreated with 400 mL of 1% NaOH in a water bath set at 90 °C and continuously stirred for 2 h. The resultant white solid was again filtered through vacuum filtration and washed with distilled water to neutralize. 350 mL NaClO and 10 mL of CH_3COOH were added to the resultant white solid and transferred to a 90 °C hot water bath with continuous stirring for 2 h. The last step was repeated for 1 h, filtered, washed with distilled water, and dried at 70 °C for 4 h.[44,45]

Preparation of cellulose nanocrystals (CNCs)

The extracted chemically purified cellulose was transferred onto a 500 mL one-neck round bottom flask, and 32% H_2SO_4 was added to the solid enough to submerge the cellulose in a 1:20 g/mL ratio. The reaction was left at room temperature for 24 h, and the resultant solution was carefully transferred into 50 mL centrifuge tubes. The samples were centrifuged at 5,000 rpm for 10 min. The supernatant was poured out carefully, distilled water was added to the resultant residue and after that centrifuged at 5,000 revolutions per minute (rpm) for 10 min. The last step was repeated four times, and the final mixture was placed in a 500 mL glass reactor onto an ultrasonic bath sonicator for 1 h at 0 °C. After ultra-sonication, the mixture was transferred onto 50 mL centrifuge tubes and washed with ethanol thrice. The recovered solid was put on a watch glass and dried in an oven at 60 °C for 1 h to a fine powder.[44,45]

Synthesis of silver nanoparticles from silver nitrate

$AgNO_3$ (0.1,360 g) and $NaHB_4$ (0.2,400 g) were transferred onto a round bottom flask, and 40 mL of deionized water was added cautiously with continuous stirring for 3 h. The resultant black solid was washed (centrifuged) three times with acetone and left to dry overnight at room temperature. The process was repeated five times to obtain enough products.

In-situ incorporation of AgNPs onto CPC and CNCs

Cellulose (0.5,003 g), 50 mL 7% NaOH, and 12% Urea solvent were transferred into the 250 mL three-neck flask. Additionally, 0.0,345 g $AgNO_3$, 0.0,604 g $NaHB_4$, and 20 mL ultra-pure water were added. The reaction was purged with nitrogen and stirred for 3 h. The resultant solid was washed three times with ethanol and left to dry overnight at 70 °C.

A similar reaction was performed using 0.4,998 g of cellulose nanocrystals, 50 mL of 7% NaOH, and 12% Urea solvent. 0.0,344 g $AgNO_3$ and 0.0,609 g $NaHB_4$ were added, followed by 20 mL of deionized water.

Characterization of wheat straw, CPC, and CNCs, and the resultant composites

Fourier transform infrared spectroscopy (FTIR)

FTIR spectroscopy was used to investigate functional groups of the wheat straw and possible changes in functional groups of Cellulose and CNCs, AgNPs, CPC-AgNPs, and CNCs- AgNPs composites. Nicolet, iS50 FT-IR (Thermo Nicolet, USA) spectrophotometer was used to perform the analysis. The spectra of the materials were collected in the transmittance mode between the 4,000 cm^{-1} to 500 cm^{-1} wavelength range.

UV–vis spectroscopy

The UV-vis spectrum of the reaction media was used to monitor the reduction of pure $Ag+$ ions after the synthesis of AgNPs and the addition of cellulosic materials. The sample's UV-vis absorption spectra of AgNPs, CPC-AgNPs, and CNCs- AgNPs composites were measured using a UV-vis spectrophotometer HITACHI U-4100 (Japan) in the 200 to 700 nm wavelength range.

Transmission electron microscopy (TEM)

The morphological features and particle sizes of the prepared CPC-AgNPs and CNCs-AgNPs were determined using a Transmission Electron Microscope (Tecnai G2 20 S-twin, Japan). After dispersing the samples in an appropriate medium, they were then placed on a copper grid covered with a carbon film. The samples were then dried before being subjected to TEM examination at an accelerating

voltage of 100-120 kV. The particle sizes were determined using ImageJ software Version 1.80.

X-ray diffraction (XRD)

An X-ray Diffractometer (Shimadzu XRD-700) was used to determine the crystallinity index of the wheat straw before and after chemical modification. Wheat straw, CPC, CNCs, CPC-AgNPs and CNCs-AgNPs were milled into powder and leveled on steel sample holders to achieve total and uniform X-ray irradiation. At 25 °C, the materials were examined using a monochromatic CuK radiation source $\lambda = 0.1{,}539$ nm with a 2 Theta angle ranging from 10° to 80°. The crystallinity index was computed using Eq. (1).

$$C_rI(\%) = \frac{I_{002} - I_{am}}{I_{002}} x100 \quad (1)$$

Where: I_{002} is the highest intensity of the 002-lattice diffraction peak and I_{am}-the- the minimum intensity dispersed by the sample's amorphous proportion.[44]

Scanning electron microscopy (SEM)

Field Emission Scanning Electron Microscopy (FE-SEM), JEOL-JSM (JEOL Ltd, Tokyo, Japan), was employed to examine and assess the morphology of CPC-AgNPs and CNCs-AgNPs. The images were captured at a voltage of 5 kV. Before SEM examination, the samples were coated with a 7 nm thick gold layer in a high vacuum environment.

Antibacterial investigation of the synthesized composites

A stock solution of 0.010 g/mL CPC-AgNPs was prepared, transferred to a 10 mL volumetric flask, and filled to the mark with 7% NaOH: 12% Urea solvent. LB Broth medium (2.5,002 g) and Agar (5.9,958 g) were prepared separately and autoclaved in a Tomy SX-700. LB Agar was dispensed onto sterile Petri dishes under a fume hood and left to solidify overnight. The plates were further inoculated with *Escherichia coli* and *Staphylococcus aureus* cultures and incubated at 37 °C. Additionally, the bacterial cultures were inoculated onto 5 mL LB Broth and set at 37 °C for two hours with constant shaking. 2 mL of 0.1%, 0.05%, and 0.025% CPC-AgNPs, CNCs-AgNPs composite was dispensed onto already prepared LB Agar, mixed and further dispensed into Petri dishes to solidify in a sterile environment. 10 µL *E. coli* and *S. aureus* cultures were further inoculated onto the plates previously prepared containing CPC-AgNPs composite, CNCs-AgNPs, and sealed with parafilm after that incubated for 24 h at 37 °C, and observations were made to determine their growth rates. A similar procedure was performed in LB Broth and inoculated bacterial cultures onto 250 mL conical flasks incubated overnight at 37 °C in a shaker incubator. The absorbance readings were taken every 30 min using a UV-Vis spectrophotometer (Thermo Scientific). The entire set-up was performed in triplicates. LB Agar and LB Broth were used as controls in each respective set-up.

The inhibitory effect experiments were carried out in triplicate, and the inhibitory effect was computed using Eq. (2) below.

$$Inhibitory\ effect\ (mm) = (CFU_c - CFU_t) \quad (2)$$

Where CFU_c is the colony-forming unit of the control and CFU_t is the colony-forming unit of the treatment.

The antibacterial activity in the solid LB agar plate was determined using the well-diffusion technique. In 100 mL of LB agar, 0.1 mL of test bacteria (10^9 CFU/mL) was injected. To each well, 50 µL of AgNP solution with concentrations of 0.1%, 0.05%, and 0.025% CPC-AgNPs, CNCs-AgNPs composite was added.

Data analysis

Origin Pro 2018 statistical software Ver. 9.5.1 generated UV-Vis, FTIR spectra, XRD graphs, TEM histograms, and growth curves.

Results and discussion

Molecular structure

The successful isolation of cellulose, cellulose nanocrystals, and synthesis of silver nanoparticles and their nanocomposites is illustrated in Figure 1. Adequate product was obtained for downstream analysis. FTIR was used to assess the structural change of wheat straw before and after chemical treatment. Figure 2a–c and Table 1 depict the Infrared spectra of wheat straw, CPC, CNCs, and the composites. A broad peak around 3,100-3,500 cm^{-1} corresponds to O-H stretching bonds, whereas a 2,800-2,950 cm-1 peak corresponds to C-H stretching bonds. The peak at 1,750 cm^{-1} corresponds to a C-O bond, generally present in ester links in hemicellulose and lignin. The peaks observed within 1,600-1,700 cm-1 show the aromatic ring contained in lignin. The peak between 1,200 and 1,300 cm^{-1} represents an out-of-plane C-O stretching in the aryl group of the lignin related to the wheat straw before chemical alteration.

The treatment of wheat straw with sodium chloride and sodium hypochlorite resulted in the elimination of the bands, FTIR spectra of CPC and CNCs (Figure 2b,c). The primary spectral bands that must be highlighted between 1,500-1,600 cm^{-1} and about 1,250 cm^{-1} are the results of the chemical treatment. The two spectral bands in these places are seen to vanish following the chemical treatments used to produce the CPC and CNCs.[44] The FTIR spectrum (Figure 2c) of CNCs is similar to that of CPC (Figure 2b), although it has sharper peaks. The peaks detected at 1,600-1,650 cm^{-1} for the CPC and CNCs are due to O-H bending caused by adsorbed water,[44] while the bands between 1,400 and 1,450 cm^{-1} are due to CH_2 interwoven in the cellulosic material. The peak at 1,050 cm^{-1} represents the C-O-C pyranose ring stretching vibration.[46] The peak seen at 900 cm^{-1} is linked to cellulosic-glycosidic connections.[47–51] These findings demonstrated that the chemical treatment of wheat straw does not alter the cellulose molecular structure.

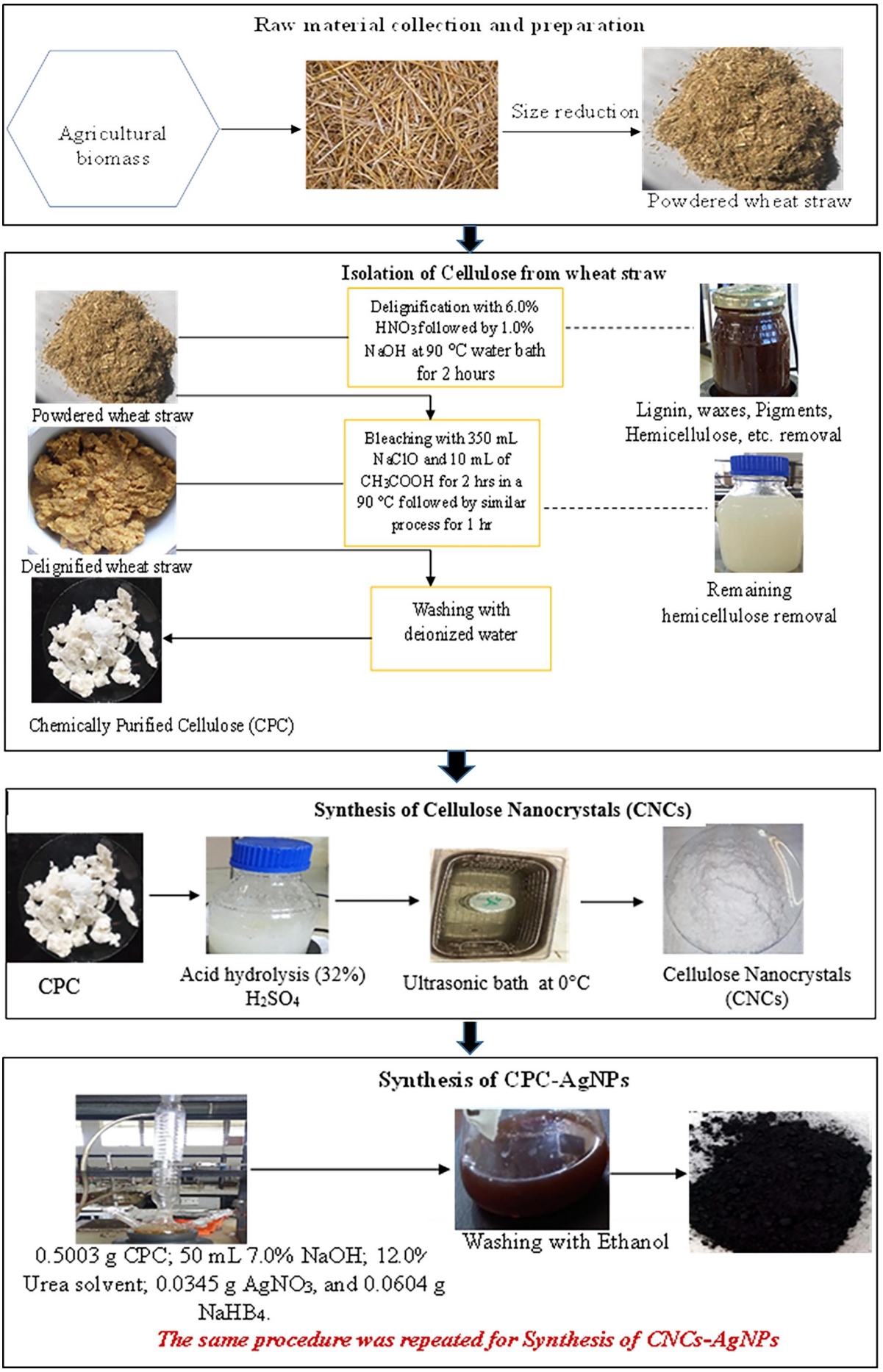

Figure 1. Isolation of Cellulose, synthesis of cellulose nanocrystals, silver nanoparticles and their nanocomposites.

In general, (Figure 2a) shows FTIR spectra of the raw material used to extract cellulose: wheat straws. The wheat straws are composed of cellulose, hemicellulose, and lignin; as a result, the functional groups of these three functional groups overlap; thus, the peaks are not so intense and broader. The shoulder observed around 1,300-1,200 cm^{-1} on the wheat spectra results from the ester and carboxylic acid group of the lignin and the hemicellulose. This shoulder peak disappears (Figure 2b) for the spectra of cellulose bleaching to show complete removal of hemicellulose and partial removal of lignin and also looking at (Figure 2c) cellulose nanocrystals after acid hydrolysis, the shoulder is seen to disappear. Looking at the spectra of wheat straws, compared to the spectra of cellulose and the nanocrystals, the peaks sharpen and become more intense. This shows that the cellulose was successfully extracted from the cellulose because there are no more overlapping peaks; thus, our cellulose is clean, and as we further do acid hydrolysis to synthesize the nanocrystals, our product becomes more cleanly and with less % lignin, therefore intense peaks.

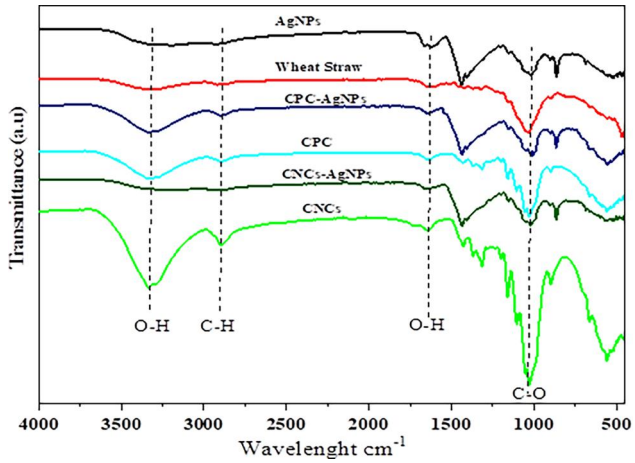

Figure 2. FTIR spectra of wheat straws (raw Material) (a), cellulose and CPC-AgNPs composite (b), CNCs and CNCs-AgNPs composite (c).

Table 1. FTIR peak absorption at different stages.

Wheat straws	Cellulose	CNCs	CNCs-AgNPs	Cellulose-AgNPs	Functional groups
3,332.32	3,334.99	3,333.78	3,245.93	3,216.05	O-H stretch
2,904.48	2,898.18	2,896.25	2,915.71	2,866.15	C-H vibration
1,651.66	1,636.16	1,640.66	1,592.36	1,635.76	O-H bond of water
1,033.42	1,053.10	1,029.94	1,017.21	1,016.06	C-O bond stretch

UV-Vis spectroscopy

Due to the surface plasmon resonance (SPR) transition, silver nanoparticles absorb light in the visible range of the electromagnetic spectrum of 380 to 450 nm. This SPR transition is responsible for the distinctive yellowish-brown color of silver nanoparticles. The UV-Vis spectra of the CPC-AgNPs composite (Figure 3a), and CNCs-AgNPs composite (Figure 3b) reveal a red shift from 382.39 to 397.73 nm and 385.52 to 399.98 nm, respectively. The same finding was reported in silver nanoparticles made by chemical reduction.[52] These wavelengths of the capped AgNPs correspond to the range of pure AgNPs, indicating the effective capping of AgNPs onto cellulose and cellulose nanocrystals.

Crystal features

The X-ray diffraction (XRD) analysis was performed to validate the crystalline form of the synthesized silver nanoparticles and the composites. The peaks at 2θ of 15.7°, 22.6°, and 35.1° in the XRD pattern of synthesized silver nanoparticles with the composites (Figure 4a,b) matched the (110), (200), and (004) crystal planes of pure cellulose.[53,54] The CNCs at 2θ of 15.3°, 22.2°, and 34.7° were also present. This showed that the cellulose from wheat straws was successfully extracted, and the nanocrystals were successfully synthesized. The four AgNPs peaks correspond to the (111), (200), (220), (311), and (222) planes of pure silver, respectively (Figure 4a,b), and to the face-centered cubic (fcc) structure of the bulk silver.[55] These peaks have 2θ values of 38.8°, 44.1°, 65.3°, and 77.8°. The synthesis of silver nanoparticles using geranium leaf extract and mushroom extract showed similar results.[56,57] This proves that silver nanoparticle synthesis was successful. The presence of AgNPs on the cellulosic materials can be seen in the x-ray diffractogram of the produced composites, which shows that the AgNPs were successfully capped onto the cellulosic materials.

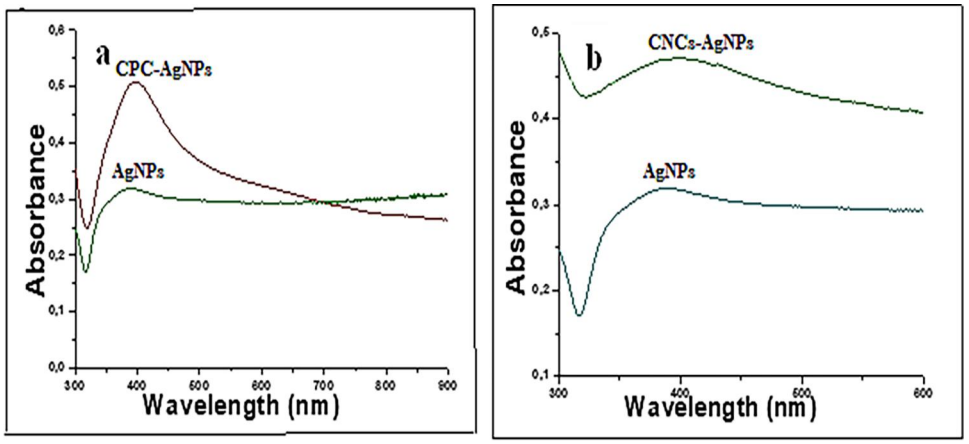

Figure 3. UV-Vis spectra of CPC-AgNPs (a), and CNCs-AgNPs composites (b).

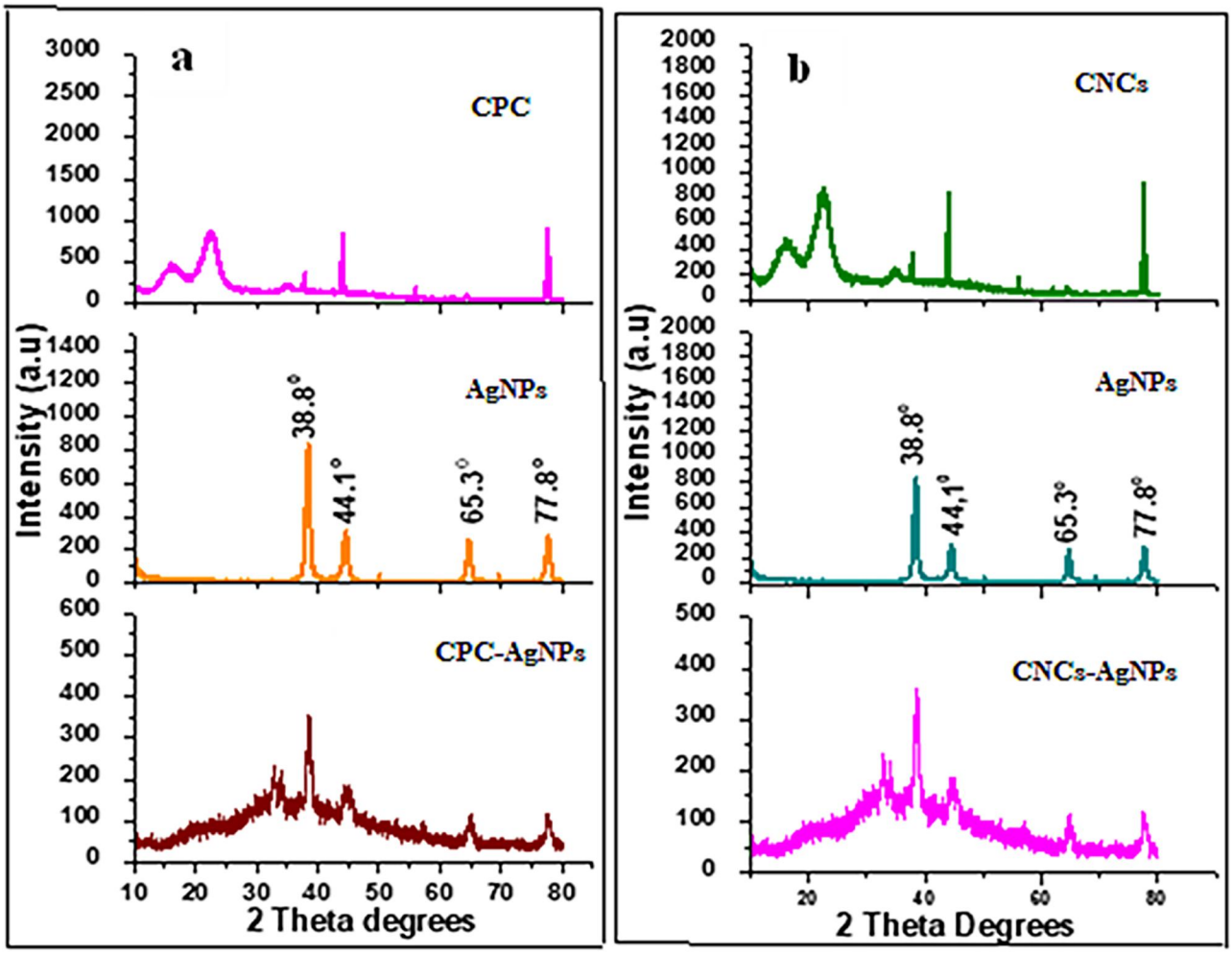

Figure 4. XRD Spectra of CPC, AgNPs and CPC-AgNPs composite (a); CNCs, AgNPs and CNCs-AgNPs nanocomposite (b).

Morphological properties

Chemical treatment of natural fibers allows for the removal of waxes, hemicelluloses, and lignin, as well as the separation of cellulose. As a result, it is critical to evaluate how the morphology changes after each step and assess the structural alterations generated in the fibers. FESEM micrographs were used to examine the surface morphology of the Cellulose and CNCs, as illustrated in (Figure 5a,b). As demonstrated in Figure 5a, alkaline treatment resulted in a severe decrease in hemicellulose content as well as a significant drop in fiber size from macro to micro. This caused fiber bundles to disperse into individual cellulose fibers with crystalline and amorphous areas. After KOH treatment, there was a considerable reduction in fiber length and diameter, with no macro- and microfibrils. Individual cellulose fiber separation increases the exposed surface area, making the fibers more sensitive to acid hydrolysis used for CNC isolation. This enables greater CNC extraction efficiency. The cellulose nanocrystals from wheat straw were rod-like (Figure 5b). Other studies obtained comparable findings for various biomass, such as rice husk[44] and sugarcane bagasse.[58] Because of its increased crystallinity, CNCs have minimal flexibility. Cellulose was produced successfully from wheat straws, and CNCs were synthesized effectively from the harvested cellulose using acid hydrolysis.

TEM images and particle size distribution of the prepared composites

Figures 6a1–b2 show the CPC-AgNPs and CNCs-AgNPs composite TEM images, respectively. Because cellulose nanocrystals are poorly contrasted against carbon support film on the TEM grid without staining, the TEM solely displays the AgNPs.[41] The two micrographs demonstrate that silver nanoparticle composites have spherical shape morphology, fine dispersion, and mean particle sizes ranging from 6 to 40 nm, with an average diameter of 16 ± 2.03 nm for CPC-AgNPs and 18 ± 1.98 nm for CNCs-AgNPs composites. The particle size of cellulosic materials has no discernible influence on particle size and shape.

Growth curves of S. aureus and E. coli

The growth curves of *S. aureus* and *E. coli* with different concentrations of the composites are illustrated in Figure 7(a_1–b_2). The graphs reveal that there was a considerable inhibitory

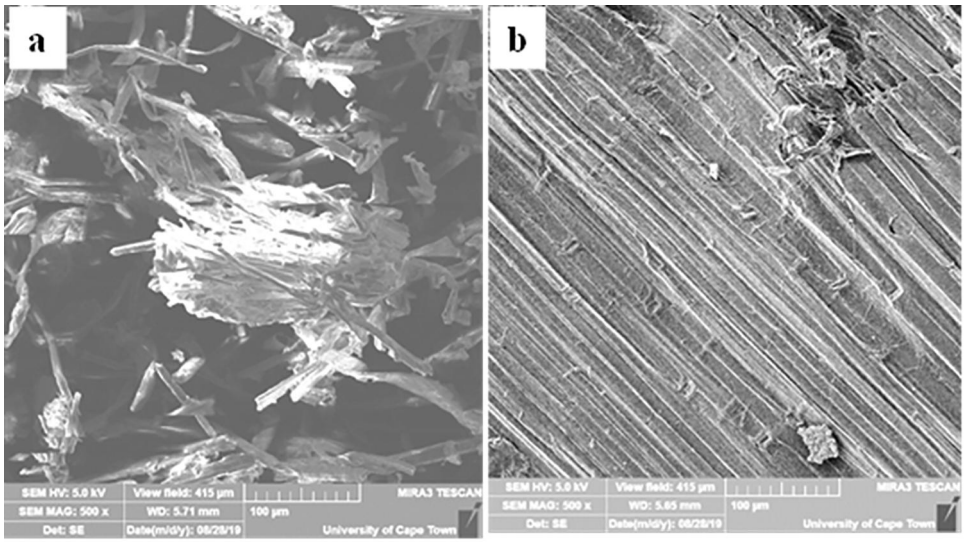

Figure 5. SEM Image of; (a) cellulose, (b) cellulose nanocrystals.

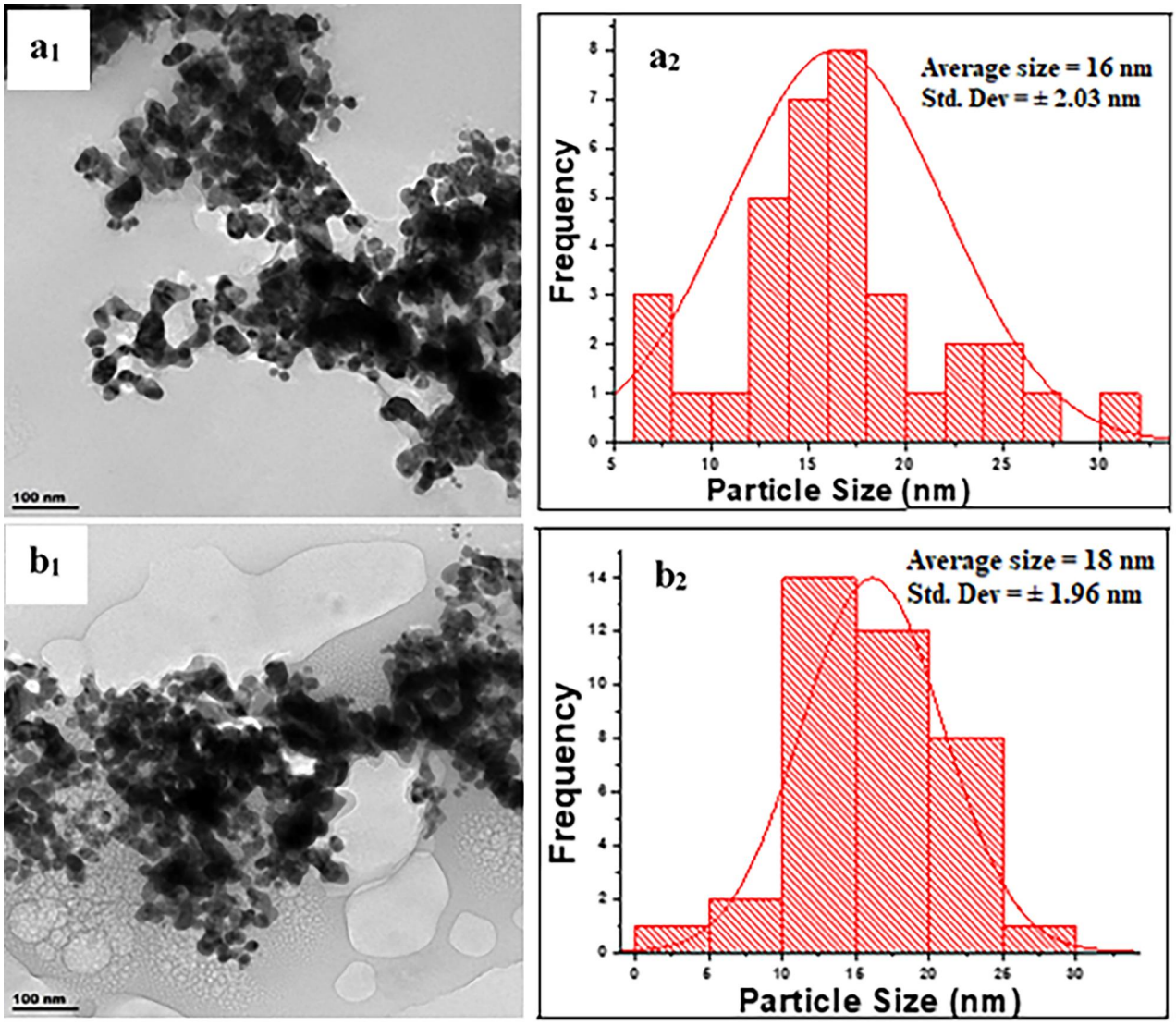

Figure 6. TEM image of CPC-AgNPs (a1), histogram of CPC-AgNPs particle size distribution (a2); CNCs-AgNPs (b1), and histogram of CNCs-AgNPs particle size distribution (b2).

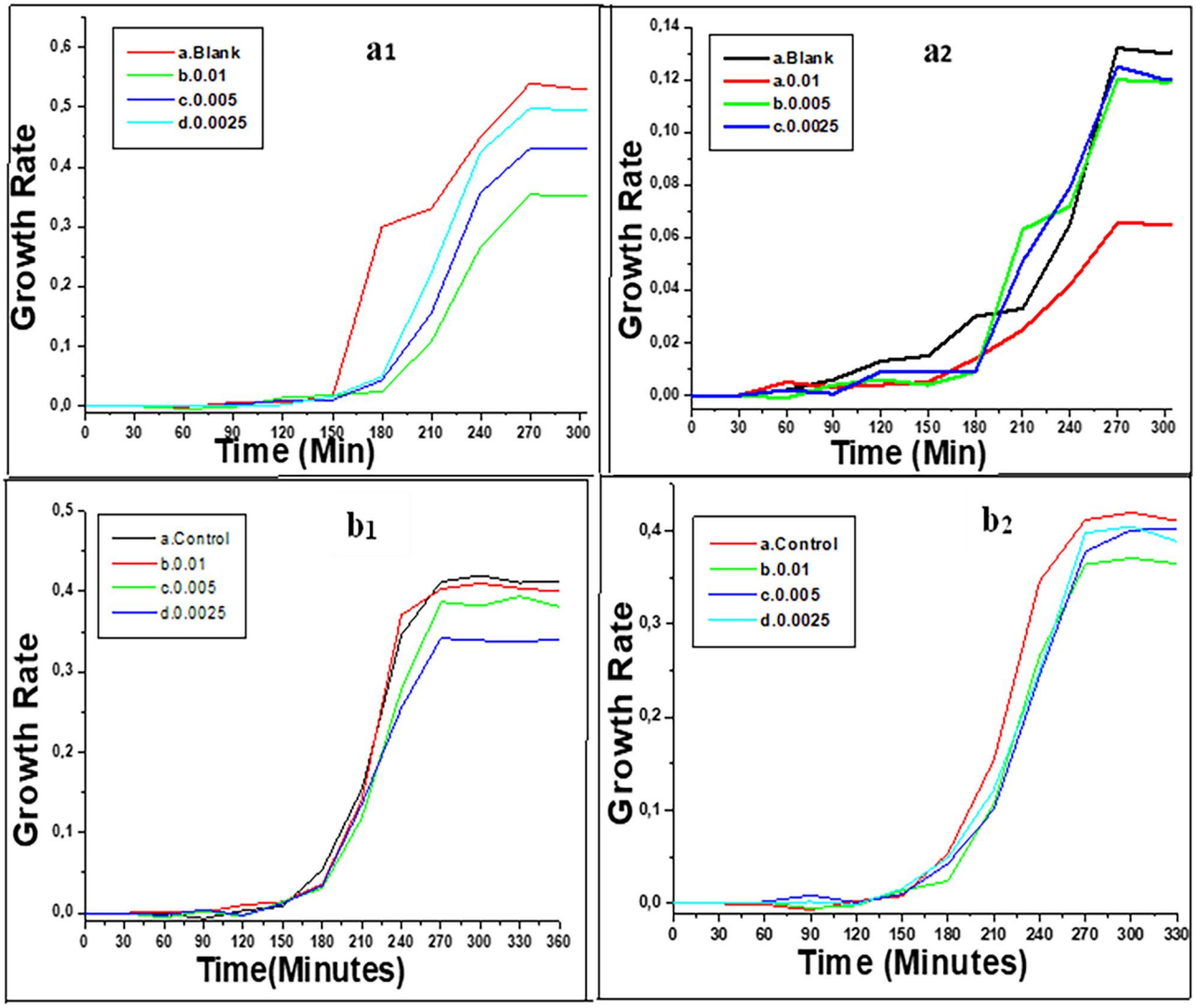

Figure 7. Growth curve of *S. aureus* (a1, a_2); growth curve of *E. coli* (b_1, b_2).

impact on bacterial growth at the greatest concentration of the studied composites. These findings imply that when bacteria are exposed to larger quantities of a certain compound, they are less likely to multiply and eventually die off. Thus, regulating or eliminating bacterial proliferation in a certain environment the phenomenon must be considered. Bacterial growth is classified into four stages: lag, exponential (log), stagnant, and decline.[59] However, the population of microorganisms does not grow during the Lag phase. The Log phase comes after the Lag phase and is characterized by an exponential increase in the number of live bacterium cells. As the bacterial population grows, resources become scarce, and harmful byproducts build. This results in the Stationary phase, where bacterial development pauses due to a shortage of nutrients and toxic chemicals. Finally, the number of live bacterial cells decreases exponentially in the Decline phase.[59,60] This is clearly illustrated by the growth curves of *S. aureus* and *E. coli* from the current work.

Inhibitory effect

The inhibition effect of the composites at different concentrations against *S. aureus* and *E. coli* cultures was investigated (Figure $8A_1$–C_2 and Table 2). Different composite concentrations were investigated, 0.01%, 0.005%, and 0.0,025%, with a control in each set-up. The inhibition zones for *E.coli* ranged from 8.05 to 12.3 mm with CPC-AgNPs and 10.02 to 13.21 for CNCs-AgNPs, while *S. aureus* ranged from 4.21 to 12.11 mm and 6.14 to 14.00 mm, respectively. The results exhibited that the inhibition of *S. aureus* increases as the concentration of the CPC-AgNPs composite decreases. This is because the CPC and AgNPs do not have a strong binding, and therefore, *S. aureus* growth was observed at lower concentrations of the composite (Figure $8A_1$). However, *E. coli* inhibition at 0.0,025% was pronounced (Figure $8A_2$) and nearly indistinguishable with the 0.005 and 0.01% of both composites. This suggests that the CPC-AgNPs composites' antibacterial activity is more effective against *E. coli* than *S. aureus*. In contrast, neither *S. aureus* nor *E. coli* bacteria grew in the CNCs-AgNPs composite at various concentrations. This is most likely owing to the cellulose nanocrystals' strong bonding with the AgNPs. The strong interaction between CNCs and AgNPs inhibited bacterial growth, it is an excellent option for antibacterial inhibition studies. The results implied that maximum inhibition

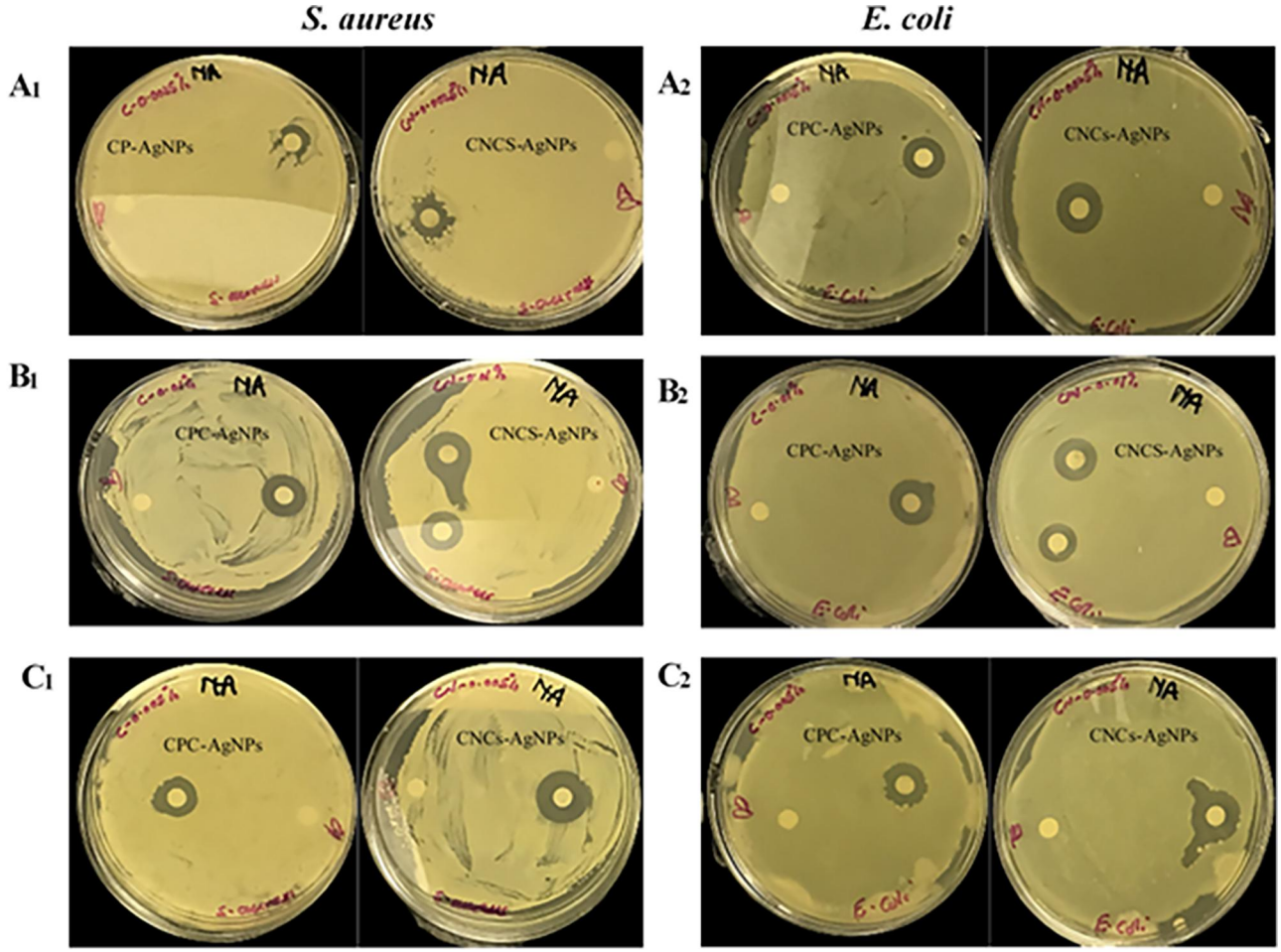

Figure 8. Inhibitory effect (A_1) 0.0,025% AgNPs composites against *S. aureus;* (A_2) 0.0,025% AgNPs composites against *E. coli;* (B_1) 0.005% composites against *S. aureus;* (B_2) 0.005% composites against *E. coli;* (C_1) 0.01% AgNPs composites against *S. aureus;* (C_2) 0.01% AgNPs composites *E. coli.*

Table 2. Antimicrobial activity of synthesized composites.

Zone of inhibition (mm)						
	CPC-AgNPs			CNCs-AgNPs		
Organism	Concentration (%)					
	0.0,025%	0.005%	0.01%	0.0,025%	0.005%	0.01%
Zone of inhibition (mm)						
E.coli	8.05 ± 20	10.05 ± 0.6	12.3 ± 22	10.02 ± 04	12.67 ± 30	13.21 ± 07
S. aureus	4.21 ± 07	9.55 ± 10	12.11 ± 03	6.14 ± 0.11	11.01 ± 0.6	14.00 ± 0.2

was obtained when treated with a 0.01% concentration of the composite as shown in Table 2. The composite's interaction with fungi's outer membrane has been shown to cause structural alterations, which may enhance membrane permeability and leaking of internal contents and instigate severe damage, ending in cell death.[61]

The current study has important implications for antibacterial research and gives useful insights into antibacterial action mechanisms. The differences in *S. aureus* and *E. coli* responses to the CPC-AgNPs composites imply that Gram-positive bacteria, may be more resistant to antibacterial drugs at low concentrations. However, the findings indicated that AgNPs capped with cellulose and cellulose nanocrystals exhibited significant antimicrobial activity and can be used in antibacterial treatments.

Conclusions

Cellulose was successfully extracted from wheat straws and then synthesized nanocrystals from the extracted cellulose by acid hydrolysis. The AgNPs were successfully capped with the cellulosic materials. The cellulosic materials containing AgNPs exhibited excellent antibacterial activity, mostly against *E. coli* than *S. aureus* at 37 °C. AgNPs capped with cellulose nanocrystals showed excellent antibacterial activity.

Acknowledgments

The authors thank the Vaal University of Technology for offering laboratory space, FTIR, UV-Vis, SEM, and XRD analysis.

Authors' contributions

Miss Shappo Tlou contributed to running the experiments, and Mr. Evans Suter contributed to sample collection, manuscript preparation, and communication. Dr. Mitema Alfred prepared bacterial media, ran the microbial experiments, and drafted part of the manuscript. Dr. Wesley Omwoyo was engaged in the article development, investigations, and data analysis. Prof. Hilary Rutto provided the chemicals, coordinated sample characterization, and proofread the draft article.

Funding

The authors have received no funding support from any institutions or organizations.

ORCID

Evans Suter http://orcid.org/0000-0003-1316-6889

Data availability statement

The data supporting this study's findings are available on request from the corresponding author. The data are not publicly available due to privacy or ethical restrictions.

Conflict of interests

All the authors declare that they do not have any competing interests.

Disclosure Statement

The authors declare there is no Complete of Interest at this study.

References

[1] Ahmad, S. A.; Das, S. S.; Khatoon, A.; Ansari, M. T.; Afzal, M.; Hasnain, M. S.; Nayak, A. K. Bactericidal Activity of Silver Nanoparticles: A Mechanistic Review. *Mater. Sci. Energy Technol.* **2020**, *3*, 756–769. DOI: 10.1016/j.mset.2020.09.002.

[2] Morones, J. R.; Elechiguerra, J. L.; Camacho, A.; Holt, K.; Kouri, J. B.; Ramírez, J. T.; Yacaman, M. J. The Bactericidal Effect of Silver Nanoparticles. *Nanotechnology* **2005**, *16*, 2346–2353. DOI: 10.1088/0957-4484/16/10/059.

[3] Durán, N.; Durán, M.; De Jesus, M. B.; Seabra, A. B.; Fávaro, W. J.; Nakazato, G. Silver Nanoparticles: A New View on Mechanistic Aspects of Antimicrobial Activity. *Nanomedicine* **2016**, *12*, 789–799. DOI: 10.1016/j.nano.2015.11.016.

[4] Tang, S.; Zheng, J. Antibacterial Activity of Silver Nanoparticles: Structural Effects. *Adv. Healthc. Mater* **2018**, *7*, e1701503. DOI: 10.1002/adhm.201701503.

[5] Gudikandula, K.; Charya Maringanti, S. Synthesis of Silver Nanoparticles by Chemical and Biological Methods and Their Antimicrobial Properties. *J. Exp. Nanosci.* **2016**, *11*, 714–721. DOI: 10.1080/17458080.2016.1139196.

[6] Garibo, D.; Borbón-Nuñez, H. A.; de León, J. N. D.; García Mendoza, E.; Estrada, I.; Toledano-Magaña, Y.; Tiznado, H.; Ovalle-Marroquin, M.; Soto-Ramos, A. G.; Blanco, A.; et al. Green Synthesis of Silver Nanoparticles Using Lysiloma Acapulcensis Exhibit High-Antimicrobial Activity. *Sci. Rep.* **2020**, *10*, 12805. DOI: 10.1038/s41598-020-69606-7.

[7] Restrepo, C. V.; Villa, C. C. Synthesis of Silver Nanoparticles, the Influence of Capping Agents, and Dependence on Size and Shape: A Review. *Environ. Nanotechnol. Monitor. Manag.* **2021**, *15*, 100428. DOI: 10.1016/j.enmm.2021.100428.

[8] Dawadi, S.; Katuwal, S.; Gupta, A.; Lamichhane, U.; Thapa, R.; Jaisi, S.; Lamichhane, G.; Bhattarai, D. P.; Parajuli, N. Current Research on Silver Nanoparticles: Synthesis, Characterization, and Applications. *J. Nanomater.* **2021**, *2021*, 1–23. DOI: 10.1155/2021/6687290.

[9] Chugh, D.; Viswamalya, V. S.; Das, B. Green Synthesis of Silver Nanoparticles with Algae and the Importance of Capping Agents in the Process. *J. Genet. Eng. Biotechnol.* **2021**, *19*, 126. DOI: 10.1186/s43141-021-00228-w.

[10] Sidhu, A. K.; Verma, N.; Kaushal, P. Role of Biogenic Capping Agents in the Synthesis of Metallic Nanoparticles and Evaluation of Their Therapeutic Potential. *Front. Nanotechnol.* **2022**, *3*, 105. DOI: 10.3389/fnano.2021.801620.

[11] Chugh, R.; Kaur, G. A Mini Review on Green Synthesis of Nanoparticles by Utilization of Musa-Balbisiana Waste Peel Extract. *Mater. Today Proc.* **2022**. DOI: https://doi.org/10.1016/j.matpr.2022.11.189.

[12] Habibi, Y. Key Advances in the Chemical Modification of Nanocelluloses. *Chem. Soc. Rev.* **2014**, *43*, 1519–1542. DOI: 10.1039/C3CS60204D.

[13] Sun, R.; Sun, X. F.; Tomkinson, J. Hemicelluloses and Their Derivatives. *Am. Chem. Soc.* **2004**, *864*, 2–22. DOI: 10.1021/bk-2004-0864.ch001.

[14] Seddiqi, H.; Oliaei, E.; Honarkar, H.; Jin, J.; Geonzon, L. C.; Bacabac, R. G.; Klein-Nulend, J. Cellulose and Its Derivatives: Towards Biomedical Applications. *Cellulose* **2021**, *28*, 1893–1931. DOI: 10.1007/s10570-020-03674-w.

[15] Liu, Y.; Ahmed, S.; Sameen, D. E.; Wang, Y.; Lu, R.; Dai, J.; Li, S.; Qin, W. A Review of Cellulose and Its Derivatives in Biopolymer-Based for Food Packaging Application. *Trends in Food Science & Technology* **2021**, *112*, 532–546. DOI: 10.1016/j.tifs.2021.04.016.

[16] Nagarajan, K. J.; Ramanujam, N. R.; Sanjay, M. R.; Siengchin, S.; Surya Rajan, B.; Sathick Basha, K.; Madhu, P.; Raghav, G. R. A Comprehensive Review on Cellulose Nanocrystals and Cellulose Nanofibers: Pre-Treatment, Preparation, and Characterization. *Polym. Compos.* **2021**, *42*, 1588–1630. DOI: 10.1002/pc.25929.

[17] Baghaei, B.; Skrifvars, M. All-Cellulose Composites: A Review of Recent Studies on Structure, Properties, and Applications. *Molecules* **2020**, *25*, 2836. DOI: 10.3390/molecules25122836.

[18] Zainul Armir, N. A.; Zulkifli, A.; Gunaseelan, S.; Palanivelu, S. D.; Salleh, K. M.; Che Othman, M. H.; Zakaria, S. Regenerated Cellulose Products for Agricultural and Their Potential: A Review. *Polymers (Basel)* **2021**, *13*, 3586. DOI: 10.3390/polym13203586.

[19] Morán, J. I.; Alvarez, V. A.; Cyras, V. P.; Vázquez, A. Extraction of Cellulose and Preparation of Nanocellulose from Sisal Fibres. *Cellulose* **2008**, *15*, 149–159. DOI: 10.1007/s10570-007-9145-9.

[20] Mokhena, T. C.; John, M. J. Cellulose Nanomaterials: New Generation Materials for Solving Global Issues. *Cellulose* **2020**, *27*, 1149–1194. DOI: 10.1007/s10570-019-02889-w.

[21] Tayeb, A. H.; Amini, E.; Ghasemi, S.; Tajvidi, M. Cellulose Nanomaterials—Binding Properties and Applications: A Review. *Molecules* **2018**, *23*, 2684. DOI: 10.3390/molecules23102684.

[22] Li, M. C.; Wu, Q.; Moon, R. J.; Hubbe, M. A.; Bortner, M. J. Rheological Aspects of Cellulose Nanomaterials: Governing Factors and Emerging Applications. *Adv. Mater.* **2021**, *33*, e2006052. DOI: 10.1002/adma.202006052.

[23] Habibi, Y.; Lucia, L. A.; Rojas, O. J. Cellulose Nanocrystals: Chemistry, Self-Assembly, and Applications. *Chem. Rev.* **2010**, *110*, 3479–3500. DOI: 10.1021/cr900339w.

[24] Chen, H.; Chen, H. Chemical Composition and Structure of Natural Lignocellulose. *Biotechnol. Lignocel.*, **2014**, 25–71 DOI: 10.1007/978-94-007-6898-7_2.

[25] Menon, V.; Rao, M. Trends in Bioconversion of Lignocellulose: Biofuels, Platform Chemicals & Biorefinery Concept. *Prog. Energy Combust. Sci.* **2012**, *38*, 522–550. DOI: 10.1016/j.pecs.2012.02.002.

[26] Sun, J. X.; Sun, X. F.; Zhao, H.; Sun, R. C. Isolation and Characterization of Cellulose from Sugarcane Bagasse. *Polym. Degrad. Stab.* **2004**, *84*, 331–339. DOI: 10.1016/j.polymdegradstab.2004.02.008.

[27] Arnata, I. W.; Suprihatin, S.; Fahma, F.; Richana, N.; Candra Sunarti, T. Cellulose Production from Sago Frond with Alkaline Delignification and Bleaching on Various Types of Bleach Agents. *Orient. J. Chem.* **2019**, *35*, 8–19. DOI: 10.13005/ojc/35Specialissue102.

[28] Manian, A. P.; Cordin, M.; Pham, T. Extraction of Cellulose Fibres from Flax and Hemp: A Review. *Cellulose* **2021**, *28*, 8275–8294. DOI: 10.1007/s10570-021-04051-x.

[29] Roy, D.; Semsarilar, M.; Guthrie, J. T.; Perrier, S. Cellulose Modification by Polymer Grafting: A Review. *Chem. Soc. Rev.* **2009**, *38*, 2046–2064. DOI: 10.1039/B808639G.

[30] Thomas, B.; Raj, M. C.; B, A. K.; H, R. M.; Joy, J.; Moores, A.; Drisko, G. L.; Sanchez, C. Nanocellulose, a Versatile Green Platform: From Biosources to Materials and Their Applications. *Chem. Rev.* **2018**, *118*, 11575–11625. DOI: 10.1021/acs.chemrev.7b00627.

[31] Kargarzadeh, H.; Huang, J.; Lin, N.; Ahmad, I.; Mariano, M.; Dufresne, A.; Thomas, S.; Gałęski, A. Recent Developments in Nano Cellulose-Based Biodegradable Polymers, Thermoplastic Polymers, and Porous Nanocomposites. *Prog. Polym. Sci.* **2018**, *87*, 197–227. DOI: 10.1016/j.progpolymsci.2018.07.008.

[32] Koshani, R.; Tavakolian, M.; van de Ven, T. G. Cellulose-Based Dispersants and Flocculants. *J. Mater. Chem. B* **2020**, *8*, 10502–10526. DOI: 10.1039/D0TB02021D.

[33] Xiang, Z.; Liu, Q.; Chen, Y.; Lu, F. Effects of Physical and Chemical Structures of Bacterial Cellulose on Its Enhancement to Paper Physical Properties. *Cellulose* **2017**, *24*, 3513–3523. DOI: 10.1007/s10570-017-1361-3.

[34] Baranwal, A.; Srivastava, A.; Kumar, P.; Bajpai, V. K.; Maurya, P. K.; Chandra, P. Prospects of Nanostructure Materials and Their Composites as Antimicrobial Agents. *Front. Microbiol.* **2018**, *9*, 422. DOI: 10.3389/fmicb.2018.00422.

[35] Ibrahim, A.; Laquerre, J. É.; Forcier, P.; Deregnaucourt, V.; Decaens, J.; Vermeersch, O. *Antimicrobial Agents for Textiles: Types, Mechanisms, and Analysis Standards*. IntechOpen Limited 5 Princes Gate Court: London, UK, **2021**; p. 13. DOI: 10.5772/interchopen.98397.

[36] Singh, P.; Ali, S. W.; Kale, R. D. Antimicrobial Nanomaterials as Advanced Coatings for Self-Sanitizing of Textile Clothing and Personal Protective Equipment. *Am. Chem. Soc.* **2023**, *8*, 8159–8171. DOI: 10.1021/acsomega.2c06343.

[37] Phanthong, P.; Reubroycharoen, P.; Hao, X.; Xu, G.; Abudula, A.; Guan, G. Nanocellulose: Extraction and Application. *Carbon Resour. Convers.* **2018**, *1*, 32–43. DOI: 10.1016/j.crcon.2018.05.004.

[38] Yin, I. X.; Zhang, J.; Zhao, I. S.; Mei, M. L.; Li, Q.; Chu, C. H. The Antibacterial Mechanism of Silver Nanoparticles and Its Application in Dentistry. *Int. J. Nanomed.* **2020**, *15*, 2555–2562. DOI: 10.2147/IJN.S246764.

[39] Hachicho, N.; Hoffmann, P.; Ahlert, K.; Heipieper, H. J. Effect of Silver Nanoparticles and Silver Ions on Growth and Adaptive Response Mechanisms of Pseudomonas putida mt-2. *FEMS Microbiol. Lett.* **2014**, *355*, 71–77. DOI: 10.1111/1574-6968.12460.

[40] Dibrov, P.; Dzioba, J.; Gosink, K. K.; Häse, C. C. Chemiosmotic Mechanism of Antimicrobial Activity of Ag+in Vibrio Cholera. *Antimicrob. Agents Chemother.* **2002**, *46*, 2668–2670. DOI: 10.1128/AAC.46.8.2668-2670.2002.

[41] Xu, Y.; Li, S.; Yue, X.; Lu, W. Review of Silver Nanoparticles (AgNPs)-Cellulose Antibacterial Composites. *BioResources* **2017**, *13*, 2150–2170. DOI: 10.15376/biores.13.1.Xu.

[42] Garza-Cervantes, J. A.; Mendiola-Garza, G.; de Melo, E. M.; Dugmore, T. I.; Matharu, A. S.; Morones-Ramirez, J. R. Antimicrobial Activity of a Silver-Micro Fibrillated Cellulose Biocomposite against Susceptible and Resistant Bacteria. *Sci. Rep.* **2020**, *10*, 7281. DOI: 10.1038/s41598-020-64127-9.

[43] Kim, J.; Kwon, S.; Ostler, E. Antimicrobial Effect of Silver-Impregnated Cellulose: Potential for Antimicrobial Therapy. *J. Biol. Eng.* **2009**, *3*, 20. DOI: 10.1186/1754-1611-3-20.

[44] Johar, N.; Ahmad, I.; Dufresne, A. Extraction, Preparation, and Characterization of Cellulose Fibers and Nanocrystals from Rice Husk. *Ind. Crops Prod.* **2012**, *37*, 93–99. DOI: 10.1016/j.indcrop.2011.12.016.

[45] Evans, S. K.; Wesley, O. N.; Nathan, O.; Moloto, M. J. Chemically Purified Cellulose and Its Nanocrystals from Sugarcane Bagasse: Isolation and Characterization. *Heliyon* **2019**, *5*, e02635. DOI: 10.1016/j.heliyon.2019.e02635.

[46] Gao, Z.; Li, N.; Chen, M.; Yi, W. Comparative Study on the Pyrolysis of Cellulose and Its Model Compounds. *Fuel Process. Technol.* **2019**, *193*, 131–140. DOI: 10.1016/j.fuproc.2019.04.038.

[47] Stuart, B. H. *Infrared Spectroscopy: Fundamentals and Applications*. John Wiley & Sons, The Atrium: West Sussex, England, **2004**.

[48] Toole, G. A.; Kačuráková, M.; Smith, A. C.; Waldron, K. W.; Wilson, R. H. FT-IR Study of the Chara Corallina Cell Wall under Deformation. *Carbohydr. Res.* **2004**, *339*, 629–635. DOI: 10.1016/j.carres.2003.11.010.

[49] Qu, X.; Wirsén, A.; Albertsson, A. C. Effect of Lactic/Glycolic Acid Side Chains on the Thermal Degradation Kinetics of Chitosan Derivatives. *Polymer* **2000**, *41*, 4841–4847. DOI: 10.1016/S0032-3861(99)00704-1.

[50] H P S, A. K.; Saurabh, C. K.; A S, A.; Nurul Fazita, M. R.; Syakir, M. I.; Davoudpour, Y.; Rafatullah, M.; Abdullah, C. K.; M Haafiz, M. K.; Dungani, R. A Review on Chitosan-Cellulose Blends and Nanocellulose Reinforced Chitosan Biocomposites: Properties and Their Applications. *Carbohydr. Polym.* **2016**, *150*, 216–226. DOI: 10.1016/j.carbpol.2016.05.028.

[51] Demuner, I. F.; Colodette, J. L.; Gomes, F. J. B.; de Oliveira, R. C. Study of LCNF and CNF from Pine and Eucalyptus Pulps. *Nordic Pulp Pap Res J.* **2020**, *35*, 670–684. DOI: 10.1515/npprj-2019-0075.

[52] Wang, H.; Qiao, X.; Chen, J.; Ding, S. Preparation of Silver Nanoparticles by Chemical Reduction Method. *Coll. Surf.* **2005**, *256*, 111–115. DOI: 10.1016/j.colsurfa.2004.12.058.

[53] Wada, M.; Heux, L.; Sugiyama, J. Polymorphism of Cellulose I Family: Reinvestigation of Cellulose IVI. *Biomacromol* **2004**, *5*, 1385–1391. DOI: 10.1021/bm0345357.

[54] Feng, X.; Meng, X.; Zhao, J.; Miao, M.; Shi, L.; Zhang, S.; Fang, J. Extraction and Preparation of Cellulose Nanocrystals from Delignate Kelp Residue: Structures and Morphological Characterization. *Cellulose* **2015**, *22*, 1763–1772. DOI: 10.1007/s10570-015-0617-z.

[55] Kora, A. J.; Sashidhar, R. B.; Arunachalam, J. Gum Kondagogu (Cochlospermum Gossypium) a Template for the Green Synthesis and Stabilization of Silver Nanoparticles with the Antibacterial Application. *Carbohyd. Polymer* **2010**, *82*, 670–679. DOI: 10.1016/j.carbpol.2010.05.034.

[56] Krithiga, N.; Rajalakshmi, A.; Jayachitra, A. Green Synthesis of Silver Nanoparticles Using Leaf Extracts of Clitoria Ternatea and Solanum Nigrum and Study of Its Antibacterial Effect against Common Nosocomial Pathogens. *J. Nanosci.* **2015**, *2015*, 1–8. DOI: 10.1155/2015/928204.

[57] Philip, D. Biosynthesis of Au, Ag, and Au–Ag Nanoparticles Using Edible Mushroom Extract. *Spectrochim. Acta A Mol. Biomol. Spectrosc.* **2009**, *73*, 374–381. DOI: 10.1016/j.saa.2009.02.037.

[58] Verma, C.; Chhajed, M.; Gupta, P.; Roy, S.; Maji, P. K. Isolation of Cellulose Nanocrystals from Different Waste Bio-Mass Collating Their Liquid Crystal Ordering with Morphological Exploration. *Int. J. Biol. Macromol.* **2021**, *175*, 242–253. DOI: 10.1016/j.ijbiomac.

[59] Maier, R. M.; Pepper, I. L. Bacterial Growth. *In Environmental Microbiology*. Academic Press: Amsterdam, Netherlands, **2015**; pp. 37–56. DOI: 10.1016/B978-0-12-394626-3.00003-X.

[60] Al-Qadiri, H. M.; Al-Alami, N. I.; Lin, M.; Al-Holy, M.; Cavinato, A. G.; Rasco, B. A. Studying the Bacterial Growth Phases Using Fourier Transform Infrared Spectroscopy and Multivariate Analysis. *J. Rapid Methods Auto. Microbiol.* **2008**, *16*, 73–89. DOI: 10.1111/j.1745-4581.2008.00117.x.

[61] Mathur, P.; Jha, S.; Ramteke, S.; Jain, N. K. Pharmaceutical Aspects of Silver Nanoparticles. *Artif. Cells Nanomed. Biotechnol.* **2018**, *46*, 115–126. DOI: 10.1080/21691401.2017.1414825.